PRL **116,** 063005 (2016) PHYSICAL REVIEW LETTERS week ending 12 FEBRUARY 2016

# Optoelectrical Cooling of Polar Molecules to Submillikelvin Temperatures

Alexander Prehn, Martin Ibrügger, Rosa Glöckner, Gerhard Rempe, and Martin Zeppenfeld[*]
*Max-Planck-Institut für Quantenoptik, Hans-Kopfermann-Strasse 1, 85748 Garching, Germany*

(Received 1 December 2015; published 10 February 2016)

We demonstrate direct cooling of gaseous formaldehyde ($H_2CO$) to the microkelvin regime. Our approach, optoelectrical Sisyphus cooling, provides a simple dissipative cooling method applicable to electrically trapped dipolar molecules. By reducing the temperature by 3 orders of magnitude and increasing the phase-space density by a factor of $\sim 10^4$, we generate an ensemble of $3 \times 10^5$ molecules with a temperature of about 420 $\mu$K, populating a single rotational state with more than 80% purity.

DOI: 10.1103/PhysRevLett.116.063005

The ability to cool atoms to ultracold temperatures has led to previously unimagined applications ranging from metrology [1] to the simulation of quantum many-body systems [2]. Cooling molecules to ultracold temperatures promises a similar variety of applications, including precision spectroscopy [3,4], investigation of fundamental physics [5,6], ultracold chemistry [7,8], study of highly anisotropic quantum gases [9,10], and quantum information [11,12]. Research with ultracold atoms has been enabled by a simple and robust technique, i.e., laser cooling. Despite substantial progress in slowing and cooling molecules directly [13–22] and in synthesizing diatomic molecules from ultracold alkali atoms [23], a similarly versatile method to cool molecules to ultracold ($T < 1$ mK) temperatures has been lacking.

An ideal cooling scheme for molecules should satisfy the following criteria: First, the technique should be simple so that it can be applied to different experiments. Second, it should be robust, without the need of permanent maintenance. Third, it should be applicable to a large variety of molecule species of interest. Fourth, and most importantly, it needs to achieve temperatures and molecule numbers which are useful for further experiments.

Here, we demonstrate that optoelectrical Sisyphus cooling [24] satisfies all of these criteria: First, it requires only a single laser, a single microwave, and a single radio-frequency (rf) source. It also requires a novel electrostatic trap [25], but this consists mainly of two microstructured electrode plates which can trivially be reproduced with modern lithographic techniques. Second, it is robust, as it is routinely operated 24 hours a day in our laboratory. Third, cooling as first demonstrated with methyl fluoride ($CH_3F$) [26] is now applied to formaldehyde ($H_2CO$) for which interesting ultracold collision experiments have been proposed [27]. Fourth, about $3 \times 10^5$ molecules can now be cooled to 0.4 mK. Although no fundamental cooling limit has been reached, two important goals are achieved: a record-large ensemble of ultracold molecules has been prepared, and a temperature has been reached which is so low that further experiments become possible, like the operation of a molecular fountain [28] or the use of microwave [29] and optical dipole traps.

Optoelectrical Sisyphus cooling proceeds in an electric trap which produces a boxlike potential for each low-field-seeking molecular state. Specifically, the trap features a homogeneous offset field in a large part of the volume and strongly increasing fields at the edges. Kinetic energy is removed by allowing molecules to repeatedly move up the electric-field gradient of the trapping potential in rotational states with a strong Stark interaction, and back down in states with weaker Stark interaction. We implement cooling in a closed scheme of trapped rovibrational states exploiting the spontaneous decay of the $v_1$ C-H stretch vibrational mode for dissipation. States are labeled with vibrational quantum number $v$ and symmetric-top rotational quantum numbers $J$, $K$, and $M$ as $|v; J, \mp K, \pm M\rangle$, with $\mp K$ chosen positive [30]. We use the rotational states characterized by $J = 3,\ 4,\ |K| = 3$. Although formaldehyde is a slightly asymmetric rotor molecule, moderately strong electric fields couple inversion-doublet rotational states such that our states essentially possess the properties of symmetric-top states [30].

The level scheme for cooling is shown in Fig. 1(a). Exciting a $\Delta M = +1$ infrared (IR) transition from states $|0; 3, 3, M < 3\rangle$ and coupling the states $|0; 3, 3, M > 0\rangle$ and $|0; 4, 3, M + 1\rangle$ with microwave (MW) radiation results in optical pumping of molecules to the strongly trapped highest $M$ sublevels. This is based on spontaneous decay from the excited states obeying the selection rules $\Delta J$, $\Delta M = 0, \pm 1$ and $\Delta K = 0$ [30]. Coupling neighboring $M$ sublevels with rf in the strong-field edge region of the trap closes the cooling cycle: transitions to more weakly trapped states in a high electric field remove kinetic energy. Losses to untrapped states are minimized by driving these transitions at a slow rate compared to the optical pumping rate to strongly trapped states [26]. The spontaneous decay rate of ~60 Hz limits the optical pumping and hence the speed of cooling. Here, we profit from formaldehyde having a four times faster vibrational decay than the previously used species methyl fluoride. Note that the rf acts on all

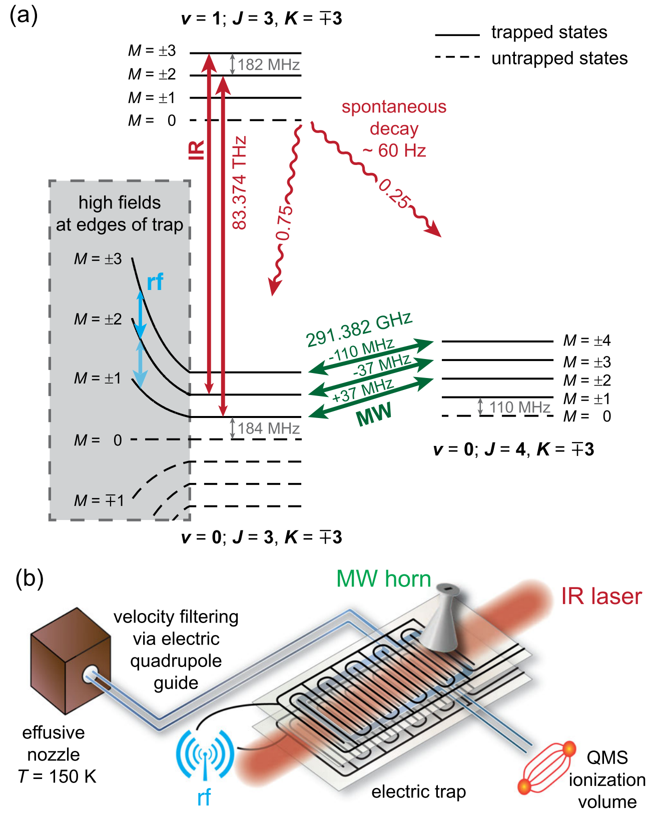

FIG. 1. (a) Level scheme for optoelectrical Sisyphus cooling as explained in the main text. Radiation (the solid arrows) couples rovibrational states, wavy arrows indicate spontaneous decay channels and their branching ratio (without resolving the $M$ substates). The Stark splitting of neighboring $M$ sublevels and transition frequencies [31,32] are given for the homogeneous-field region of the trap ($V_{\mathrm{trap}} = \pm 1500$ V). (b) Experimental setup. Molecules are loaded into the trap from a velocity-filtered thermal source ($T \approx 150$ K) via an electric quadrupole guide [25,33]. The radiation fields needed for cooling are applied as indicated. A second guide brings molecules to a quadrupole mass spectrometer (QMS), where a time-resolved count rate is recorded.

molecules, although the potential energy curves and transitions in the edge region of the trap are only sketched for one set of states in the figure.

The experimental setup is shown and explained in Fig. 1(b). Its key part is the electrostatic trap, where molecules are trapped between a pair of microstructured capacitor plates (spaced 3 mm) and a surrounding electrode [25]. Alternating high voltages $\pm V_{\mathrm{trap}}$, applied to adjacent electrodes of the microstructure, produce strong trapping fields. To suppress so-called Majorana flips to untrapped states and to spectroscopically separate the rotational $M$ substates, an offset electric field is created by applying additional voltages $\pm V_{\mathrm{offset}}$ across the capacitor. This yields a homogeneous offset field in the center of the trap, with a finite roughness owing to $\pm V_{\mathrm{trap}}$ [25]. Except for the detection of molecules, $\pm V_{\mathrm{offset}}$ always equals 5% of $\pm V_{\mathrm{trap}}$, thus ensuring a fixed relation of offset and trapping fields. The unique design offers long storage times for polar molecules. Uncooled molecules can be stored with a $1/e$ decay time on the order of 10 s [25], while for cooled molecules it can be as long as a minute [30].

The actual shape of the trap potential strongly influences both the cooling sequence and the determination of the final temperature. For example, we later subtract the offset potential energy from the measured total energy of the molecules to determine their kinetic energy based on the assumption of a boxlike potential. This simple picture is only valid if the kinetic energy of the molecules is sufficiently larger than the roughness of the offset field of the electric box. Therefore, we investigate the potential landscape in detail by measuring electric-field distributions. Evidently, a boxlike potential with a large homogeneous-field region translates to a strongly peaked electric-field distribution, with the width of the peak giving the roughness of the offset. The distribution is measured by performing Stark spectroscopy on the single MW transition coupling the states $|0;3,3,3\rangle$ and $|0;4,3,4\rangle$, similar to previous work [34]. The line shape of the measured depletion spectrum is primarily given by Stark broadening and thus allows us to extract the probability for a specific electric field to occur in the trap [34].

The measured and simulated electric-field distributions for the four trap-voltage configurations used for the experiments in this Letter are plotted in Fig. 2. The configurations in Figs. 2(a)–2(c) are used during cooling, whereas Figs. 2(c) and 2(d) are relevant for the determination of the final temperature. Narrow peaks confirm that the electric fields are indeed homogeneous in a large fraction of the trap volume. The simulation which is very briefly described in the Supplemental Material [30] predicts the peak position and the overall shape of the distribution quite well. In a perfect trap, the field distributions are expected to scale with the applied trap voltage. However, the relative widths of the distributions increase and a slight shift of the peak is observable for small voltages. In particular, halving the voltage from $V_{\mathrm{trap}} = \pm 100$ V to $V_{\mathrm{trap}} = \pm 50$ V [see Figs. 2(c) and 2(d)] still approximately halves the strength of the homogeneous field, but it does not narrow the width noticeably anymore. We attribute this effect to the existence of surface charges on the microstructured capacitor plates [30]. Note that the measured distribution is convolved with the probability for molecules to be at a given potential energy, which mainly influences the high-field tail of the distribution [34].

The aspects of the boxlike potential which are relevant to this work can be captured by two parameters of the measured electric-field distributions. First, the center of the peak defines the homogeneous offset electric field. This allows calculation of the Stark splitting of $M$ sublevels in this region as $f_{\mathrm{offset}} = (\mathcal{E}\mu/h)[K/J(J+1)]$, with electric-field strength $\mathcal{E}$, electric dipole moment $\mu$, and the

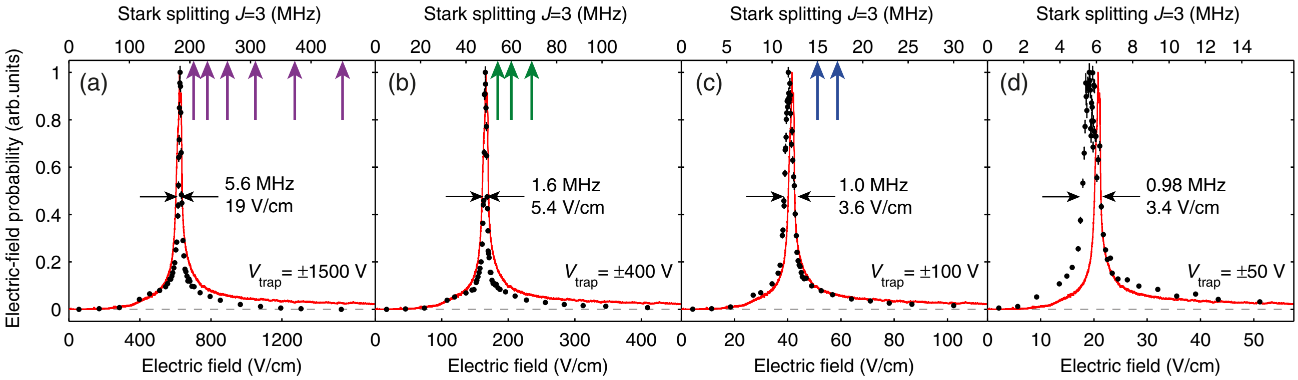

FIG. 2. Measured (dots) and simulated (solid line; see the Supplemental Material [30]) electric-field distribution in the trap, both normalized to the maximum. Error bars represent the $1\sigma$ statistical error. We indicate the FWHM of the measured distributions. The applied trap voltages were varied over a factor of 30 (see the lower right corner of the panels). The upper horizontal axes show the Stark splitting of the states $|0;3,3,M\rangle$ in frequency units. Configurations (a)–(c) are used during cooling and arrows indicate the frequencies of the rf coupling ($f_{\mathrm{rf}}$) applied sequentially for cooling. Panels (c),(d) are relevant for the determination of the final kinetic energy.

rotational quantum numbers (cf. the upper horizontal axes of Fig. 2). Consequently, $Mf_{\mathrm{offset}}$ defines the potential energy offset, which we later subtract, for each low-field-seeking state. Second, the width of the field distribution compared to the kinetic energy of the molecules defines whether we can treat the potential as boxlike in the first place. Molecules loaded into the trap initially can reach electric fields above 10 kV/cm, and the potential is then clearly boxlike.

The previous results can now be used to discuss the effect of the rf on cooling. The amount of kinetic energy extracted per induced rf transition is given by the applied rf frequency $f_{\mathrm{rf}}$, and by $f_{\mathrm{offset}}$ as $\Delta E \sim h(f_{\mathrm{rf}} - f_{\mathrm{offset}})$. On one hand, a larger $f_{\mathrm{rf}}$ leads to more cooling per transition. On the other hand, the molecules have to possess sufficient kinetic energy to reach the high electric fields where the rf is resonant to allow for a transition. Consequently, $f_{\mathrm{rf}}$ has to be reduced as cooling advances. We chose to lower $(f_{\mathrm{rf}} - f_{\mathrm{offset}})$ stepwise in factors of $\sim\sqrt{2}$ every 2 s, corresponding to about one induced transition per applied frequency [26].

In the course of cooling, $f_{\mathrm{rf}}$ approaches $f_{\mathrm{offset}}$ and $(f_{\mathrm{rf}} - f_{\mathrm{offset}})$ becomes comparable to the width of the electric-field distribution. This can be seen in Fig. 2(a), where vertical arrows denote the last six $f_{\mathrm{rf}}$ applied with the initial trap-voltage configuration. Thus, the molecules do not move in a well-defined box potential anymore and spend significant time in not very well-defined isolated regions of low electric field. To maintain a simple boxlike potential, we ramp down the trap voltages adiabatically twice during cooling to $V_{\mathrm{trap}} = \pm 400$ V and $V_{\mathrm{trap}} = \pm 100$ V. This shifts the offset of the potential, $f_{\mathrm{offset}}$, and reduces the width of the field distribution as intended. We perform, in total, five more cooling steps in a reduced trap potential [the arrows in Figs. 2(b) and 2(c)].

The preceding discussion leads to the following sequence to cool and detect a sample of molecules,

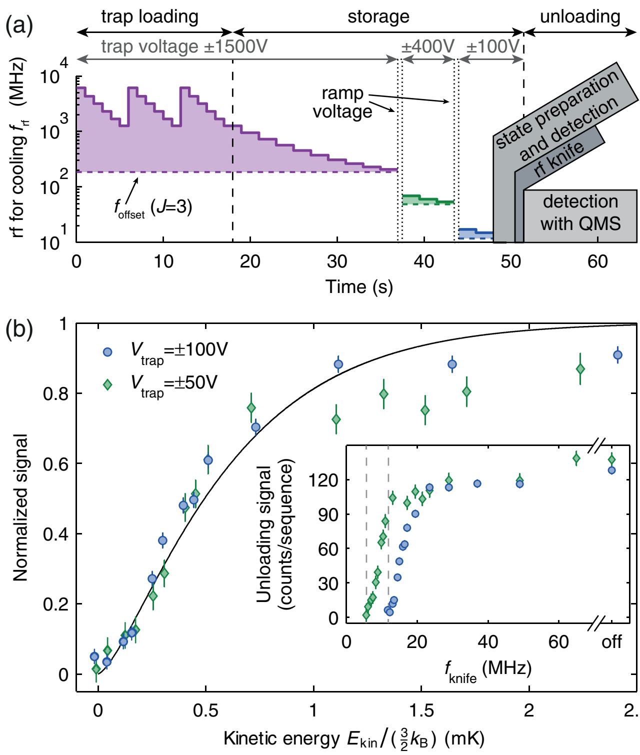

FIG. 3. (a) Experimental sequence. The rf applied for cooling is plotted together with the trapping sequence vs time. The dashed horizontal lines mark $f_{\mathrm{offset}}$ for $J = 3$. The experimental steps performed after cooling are explained in the main text. (b) Measurement of the kinetic energy via rf knife-edge filters. The inset shows the signal of molecules remaining in the states $|0;3,3,3\rangle$ vs $f_{\mathrm{knife}}$, with the filter applied with two distinct trap voltages. The dashed lines mark the potential energy offset $f_{\mathrm{offset}}$, which is 11.9 MHz (5.7 MHz) for $V_{\mathrm{trap}} = \pm 100$ V ($V_{\mathrm{trap}} = \pm 50$ V). The main panel plots the same data vs kinetic energy, normalized to the signal without a rf knife and on a narrower horizontal scale. The solid line represents an integrated Boltzmann distribution for a temperature of 420 $\mu$K. Error bars denote the $1\sigma$ statistical error.

consisting of six parts, as depicted in Fig. 3(a). First, molecules are continuously loaded into the trap (voltage ±1500 V) for 18 s, with cooling already applied. The lifetime of molecules in the trap increases substantially for colder molecules [26]. Therefore, cooling as many hot molecules entering the trap at different times and with varying energy as fast as possible to an energy with a decent lifetime is desirable. To achieve this, we apply and cycle six $f_{\mathrm{rf}}$ during loading. Then, the ensemble is stored and further cooled while reducing $f_{\mathrm{rf}}$ and lowering the trapping potential as described above. After cooling, the molecules are prepared in a single rotational state. Thus, the trap potential is identical for all observed molecules. Specifically, we optically pump to the state $|0;3,3,3\rangle$ [30,35] and utilize a rotational-state-detection technique [30,34]. Next, the energy of the molecular ensemble is probed by applying a strong rf field that acts as a knife-edge filter and only eliminates hotter molecules (see below). Finally, the molecules are unloaded from the trap and counted with a quadrupole mass spectrometer (QMS). Presently, very cold molecules can only be extracted efficiently from the trap if the ensemble is parametrically heated before unloading [30]. The reason for heating is not fundamental but technical: possibly due to disturbed electric fields created by surface charges or a misalignment at the transition from the trap to the guide, slow molecules are lost before they reach the detector [30].

The rf knife-edge filter employed for measuring the energy of the molecules works as follows. A strong rf field drives $\Delta M = -1$, $\Delta K = 0$ transitions to the untrapped $M = 0$ states and quickly depletes all those molecules from the trap possessing sufficient energy to reach the (higher) electric field where the rf is resonant. Hence, a rf knife with a frequency $f_{\mathrm{knife}}$ truncates the energy distribution of the molecules at a known total energy and leaves only less energetic molecules in the trap. Scanning $f_{\mathrm{knife}}$ and observing the molecule signal thus yields an integrated energy distribution of the trapped molecules. Note that due to formaldehyde being an asymmetric rotor additionally $\pm K \to \mp K$ transitions can be induced in a lower electric field [30]. These transitions require orders of magnitude higher rf power and are thus well separated from the desired energy-dependent filtering [30].

The inset of Fig. 3(b) shows the remaining signal in the state $|0;3,3,3\rangle$ vs $f_{\mathrm{knife}}$. To address the issue of offset subtraction, we measure the energy distribution for two distinct trap voltages: $V_{\mathrm{trap}} = \pm 100$ V, the trap potential present in the final two cooling steps, and $V_{\mathrm{trap}} = \pm 50$ V. In both cases, a knife with $f_{\mathrm{knife}} \approx f_{\mathrm{offset}}$, resonant to the offset of the boxlike potential, depletes all molecules from the trap as expected. With rising knife frequency we observe steeply rising flanks which are clearly separated due to the different potential energy offsets. At higher frequencies a slight further increase towards the data point without a rf knife is visible. Those molecules, about 10% of the ensemble, were not cooled efficiently in the last cooling steps and therefore have a much higher kinetic energy than the vast majority of the fully cooled ones. If necessary, this high-energy part of the molecular ensemble could be removed from the trap by applying a suitable rf knife.

To obtain a kinetic energy distribution from the measurement, the contribution of potential energy has to be considered. As we can treat the trap potential as boxlike, we account for this by subtracting the offset potential energy, $Mhf_{\mathrm{offset}}$, extracted from the measured electric-field distributions [see above, Figs. 2(c) and 2(d)]. We verified that systematic errors caused by this simple approach are smaller than our statistical uncertainty. Consequently, we find for the kinetic energy $E_{\mathrm{kin}} = Mh(f_{\mathrm{knife}} - f_{\mathrm{offset}})$. The measured data with the offset potential energy subtracted is shown in the main panel of Fig. 3(b). Normalized to the signal without a rf knife, the two curves obtained with different trap voltages show a good overlap. This is expected from the fact that the subtraction of a well-defined offset potential energy should not influence the kinetic energy distribution.

From the data, we compute a median kinetic energy of $E_{\mathrm{kin}}/(\frac{3}{2}k_B) = (420 \pm 90)\ \mu\mathrm{K}$ with the factor of 3 accounting for the three translational degrees of freedom in a box potential. The energy at which half of the molecular ensemble is depleted was determined by fitting the curve for $V_{\mathrm{trap}} = \pm 100$ V with a linear slope in the vicinity of this kinetic energy. As a comparison, we additionally plot a Boltzmann distribution for a temperature of 420 $\mu$K. The good agreement of thermal distribution and measured data supports our interpretation of $E_{\mathrm{kin}}/(\frac{3}{2}k_B)$ as an approximate temperature.

The produced molecular ensemble is both large and internally pure. Calibrating the sensitivity of the QMS, we determine the number of cooled molecules unloaded from the trap to be $3 \times 10^5$, accurate to within a factor of 2 [30]. We measure $(83 \pm 3)\%$ of the molecules to populate the single rotational state $|0;3,3,3\rangle$ [30]. The result can be compared to an uncooled reference ensemble: molecules unloaded from the trap after 18 s of trap loading and two seconds of storage without any manipulation, resulting in $10^6$ molecules with 460 mK in the states $|0;3,3,M\rangle$. This comparison yields a reduction of kinetic energy by a factor of 1000 and an increase in phase-space density of about $10^4$.

With the simple and robust technique of optoelectrical Sisyphus cooling, we produced a large ensemble of trapped ultracold molecules. In principle, further cooling with the same method is possible, if the technical issue with the surface charges, which broaden the electric fields in the present setup, is solved. Additionally, larger ensembles of molecules could be produced by loading buffer-gas cooled [36] and decelerated [18] molecules into our trap. We note that our method relies on rather general properties of polar molecules and should thus be applicable to a wide range of additional species [24].

The temperature and ensemble size reached enable further experiments. The low velocity of the cooled molecules of ∼0.6 m/s makes fountain experiments feasible [28]. The ability to control the final kinetic energy and rotational state is an ideal starting point for collision studies and the investigation of cold and ultracold chemistry [7,8]. Finally, the temperature achieved should allow efficient transfer to a microwave [29] or optical trap where molecules can be held in their absolute ground state, a prerequisite for sympathetic [37,38] or evaporative cooling.

*Note added.*—Similar results on the direct cooling of molecules to submillikelvin temperatures using a radiofrequency magneto-optical trap are reported in Ref. [39].

---

[*] Martin.Zeppenfeld@mpq.mpg.de

[1] J. Huang, S. Wu, H. Zhong, and C. Lee, Quantum metrology with cold atoms, in *Annual Review of Cold Atoms and Molecules*, Vol. 2 (World Scientific, Singapore, 2014), Chap. 7, p. 365.

[2] I. Bloch, J. Dalibard, and W. Zwerger, Many-body physics with ultracold gases, Rev. Mod. Phys. **80**, 885 (2008).

[3] S. Truppe, R. J. Hendricks, S. K. Tokunaga, H. J. Lewandowski, M. G. Kozlov, C. Henkel, E. A. Hinds, and M. R. Tarbutt, A search for varying fundamental constants using hertz-level frequency measurements of cold CH molecules, Nat. Commun. **4**, 2600 (2013).

[4] M. Schnell and J. Küpper, Tailored molecular samples for precision spectroscopy experiments, Faraday Discuss. **150**, 33 (2011).

[5] J. Baron, W. C. Campbell, D. DeMille, J. M. Doyle, G. Gabrielse, Y. V. Gurevich, P. W. Hess, N. R. Hutzler, E. Kirilov, I. Kozyryev, B. R. O'Leary, C. D. Panda, M. F. Parsons, E. S. Petrik, B. Spaun, A. C. Vutha, and A. D. West (ACME Collaboration), Order of magnitude smaller limit on the electric dipole moment of the electron, Science **343**, 269 (2014).

[6] D. DeMille, S. B. Cahn, D. Murphree, D. A. Rahmlow, and M. G. Kozlov, Using Molecules to Measure Nuclear Spin-Dependent Parity Violation, Phys. Rev. Lett. **100**, 023003 (2008).

[7] M. T. Bell and T. P. Softley, Ultracold molecules and ultracold chemistry, Mol. Phys. **107**, 99 (2009).

[8] B. K. Stuhl, M. T. Hummon, and J. Ye, Cold state-selected molecular collisions and reactions, Annu. Rev. Phys. Chem. **65**, 501 (2014).

[9] M. A. Baranov, M. Dalmonte, G. Pupillo, and P. Zoller, Condensed matter theory of dipolar quantum gases, Chem. Rev. **112**, 5012 (2012).

[10] M. L. Wall, K. Maeda, and L. D. Carr, Realizing unconventional quantum magnetism with symmetric top molecules, New J. Phys. **17**, 025001 (2015).

[11] A. André, D. DeMille, J. M. Doyle, M. D. Lukin, S. E. Maxwell, P. Rabl, R. J. Schoelkopf, and P. Zoller, A coherent all-electrical interface between polar molecules and mesoscopic superconducting resonators, Nat. Phys. **2**, 636 (2006).

[12] Q. Wei, S. Kais, B. Friedrich, and D. Herschbach, Entanglement of polar symmetric top molecules as candidate qubits, J. Chem. Phys. **135**, 154102 (2011).

[13] M. Quintero-Pérez, T. E. Wall, S. Hoekstra, and H. L. Bethlem, Preparation of an ultra-cold sample of ammonia molecules for precision measurements, J. Mol. Spectrosc. **300**, 112 (2014).

[14] J. F. Barry, D. J. McCarron, E. B. Norrgard, M. H. Steinecker, and D. DeMille, Magneto-optical trapping of a diatomic molecule, Nature (London) **512**, 286 (2014).

[15] D. Patterson and J. M. Doyle, A slow, continuous beam of cold benzonitrile, Phys. Chem. Chem. Phys. **17**, 5372 (2015).

[16] E. Narevicius and M. G. Raizen, Toward cold chemistry with magnetically decelerated supersonic beams, Chem. Rev. **112**, 4879 (2012).

[17] S. Y. van de Meerakker, H. L. Bethlem, N. Vanhaecke, and G. Meijer, Manipulation and control of molecular beams, Chem. Rev. **112**, 4828 (2012).

[18] S. Chervenkov, X. Wu, J. Bayerl, A. Rohlfes, T. Gantner, M. Zeppenfeld, and G. Rempe, Continuous Centrifuge Decelerator for Polar Molecules, Phys. Rev. Lett. **112**, 013001 (2014).

[19] H.-I Lu, I. Kozyryev, B. Hemmerling, J. Piskorski, and J. M. Doyle, Magnetic Trapping of Molecules via Optical Loading and Magnetic Slowing, Phys. Rev. Lett. **112**, 113006 (2014).

[20] S. Merz, N. Vanhaecke, W. Jäger, M. Schnell, and G. Meijer, Decelerating molecules with microwave fields, Phys. Rev. A **85**, 063411 (2012).

[21] S. Marx, D. Adu Smith, M. J. Abel, T. Zehentbauer, G. Meijer, and G. Santambrogio, Imaging Cold Molecules on a Chip, Phys. Rev. Lett. **111**, 243007 (2013).

[22] S. D. Hogan, C. Seiler, and F. Merkt, Rydberg-State-Enabled Deceleration and Trapping of Cold Molecules, Phys. Rev. Lett. **103**, 123001 (2009).

[23] K.-K. Ni, S. Ospelkaus, M. H. G. de Miranda, A. Pe'er, B. Neyenhuis, J. J. Zirbel, S. Kotochigova, P. S. Julienne, D. S. Jin, and J. Ye, A high phase-space-density gas of polar molecules, Science **322**, 231 (2008).

[24] M. Zeppenfeld, M. Motsch, P. W. H. Pinkse, and G. Rempe, Optoelectrical cooling of polar molecules, Phys. Rev. A **80**, 041401 (2009).

[25] B. G. U. Englert, M. Mielenz, C. Sommer, J. Bayerl, M. Motsch, P. W. H. Pinkse, G. Rempe, and M. Zeppenfeld, Storage and Adiabatic Cooling of Polar Molecules in a Microstructured Trap, Phys. Rev. Lett. **107**, 263003 (2011).

[26] M. Zeppenfeld, B. G. U. Englert, R. Glöckner, A. Prehn, M. Mielenz, C. Sommer, L. D. van Buuren, M. Motsch, and G. Rempe, Sisyphus cooling of electrically trapped polyatomic molecules, Nature (London) **491**, 570 (2012).

[27] E. R. Hudson, C. Ticknor, B. C. Sawyer, C. A. Taatjes, H. J. Lewandowski, J. R. Bochinski, J. L. Bohn, and J. Ye, Production of cold formaldehyde molecules for study and control of chemical reaction dynamics with hydroxyl radicals, Phys. Rev. A **73**, 063404 (2006).

[28] H. L. Bethlem, M. Kajita, B. Sartakov, G. Meijer, and W. Ubachs, Prospects for precision measurements on ammonia molecules in a fountain, Eur. Phys. J. Spec. Top. **163**, 55 (2008).

[29] D. DeMille, D. R. Glenn, and J. Petricka, Microwave traps for cold polar molecules, Eur. Phys. J. D **31**, 375 (2004).

[30] See Supplemental Material at http://link.aps.org/supplemental/10.1103/PhysRevLett.116.063005 for experimental details.

[31] R. Cornet and G. Winnewisser, A precise study of the rotational spectrum of formaldehyde $H_2{}^{12}C^{16}O$, $H_2{}^{13}C^{16}O$, $H_2{}^{12}C^{18}O$, $H_2{}^{13}C^{18}O$, J. Mol. Spectrosc. **80**, 438 (1980).

[32] L. Rothman *et al.*, The HITRAN 2008 molecular spectroscopic database, J. Quant. Spectrosc. Radiat. Transfer **110**, 533 (2009).

[33] T. Junglen, T. Rieger, S. A. Rangwala, P. W. H. Pinkse, and G. Rempe, Slow ammonia molecules in an electrostatic quadrupole guide, Eur. Phys. J. D **31**, 365 (2004).

[34] R. Glöckner, A. Prehn, G. Rempe, and M. Zeppenfeld, Rotational state detection of electrically trapped polyatomic molecules, New J. Phys. **17**, 055022 (2015).

[35] R. Glöckner, A. Prehn, B. G. U. Englert, G. Rempe, and M. Zeppenfeld, Rotational Cooling of Trapped Polyatomic Molecules, Phys. Rev. Lett. **115**, 233001 (2015).

[36] L. D. van Buuren, C. Sommer, M. Motsch, S. Pohle, M. Schenk, J. Bayerl, P. W. H. Pinkse, and G. Rempe, Electrostatic Extraction of Cold Molecules from a Cryogenic Reservoir, Phys. Rev. Lett. **102**, 033001 (2009).

[37] S. K. Tokunaga, W. Skomorowski, P. S. Żuchowski, R. Moszynski, J. M. Hutson, E. A. Hinds, and M. R. Tarbutt, Prospects for sympathetic cooling of molecules in electrostatic, ac and microwave traps, Eur. Phys. J. D **65**, 141 (2011).

[38] J. J. Lutz and J. M. Hutson, Reactions between cold methyl halide molecules and alkali-metal atoms, J. Chem. Phys. **140**, 014303 (2014).

[39] E. B. Norrgard, D. J. McCarron, M. H. Steinecker, M. R. Tarbutt, and D. DeMille, preceding Letter, Submillikelvin Dipolar Molecules in a Radio-Frequency Magneto-optical Trap, Phys. Rev. Lett. **116**, 063004 (2016).